Modal Behavior of Hemispheric Sea Ice Covers

Per Gloersen and Norden Huang

Oceans and Ice Branch, Laboratory for Hydrospheric Processes

NASA Goddard Space Flight Center

Greenbelt, Maryland 20771

Zheng Shen

Division of Engineering Science

California Institute of Technology

Pasadena, California 91125

Summary

A newly-formulated 18.2-year ice concentration time series for the entire Arctic and Antarctic ice covers, as well as for previously defined subregions consisting of 5 sectors in the Antarctic and 9 regions in the Arctic is analyzed by means of a recently patented procedure called "Empirical Mode Decompostion", with emphasis on periodicities greater than the annual cycle. Quasibiennial and quasiquadrennial oscillations observed with a different technique and reported earlier for the first 8.8 years of this time series were also observed in the present series. However, the intrinsic modes are not monochromatic; they feature frequency as well as amplitude modulation within their respective frequency bands. Modal periods of up to 18 years are observed and periods about twice as long are hinted at, with important implications for the trend analyses published earlier.

Approval Request entries:

1. Modal Behavior of Hemispheric Sea Ice Covers

Au: Per Gloersen (ξ 7.)

Norden Huang

Zheng Shen
3. Journal
5. JGR oceans

6. No, Yes, No

Modal Behavior of Hemispheric Sea Ice Covers

Per Gloersen and Norden Huang

Oceans and Ice Branch, Laboratory for Hydrospheric Processes

NASA/Goddard Space Flight Center

Greenbelt, Maryland 20117

Zheng Shen

Division of Engineering Science

California Institute of Technology

Pasadena, California 91125

Significant Findings:

Recent papers have described 18-year trends and annual oscillations in the Arctic and Antarctic sea ice extents, areas, and enclosed open water areas based on a newly-formulated 18.2-year ice concentration time series. This time series includes data for the entire Arctic and Antarctic ice covers, as well as for previously defined subregions consisting of 5 sectors in the Antarctic and 9 regions in the Arctic. It was obtained by fine-tuning the sea ice algorithm tie points individually for each of the four sensors used to acquire the data. In this paper, we extend these analyses to an examination of the intrinsic modes of these time series, obtained by means of Empirical Mode Decomposition, with emphasis on periodicities greater than the annual cycle. Quasibiennial and quasiquadrennial oscillations observed with a different technique and reported earlier for the first 8.8 years of this time series were also observed in the present series. However, the intrinsic modes were not monochromatic; they feature frequency as well as amplitude modulation within their respective frequency bands. Modal periods of up to 18 years are observed, with important implications for the trend analyses published earlier.

970

Modal Behavior of Hemispheric Sea Ice Covers

Per Gloersen and Norden Huang

Oceans and Ice Branch, Laboratory for Hydrospheric Processes

NASA/Goddard Space Flight Center

Greenbelt, Maryland 20117

Zheng Shen

Division of Engineering Science

California Institute of Technology

Pasadena, California 91125

Strategic Plan

This research is directly related to Item 4 of the MPTE Enterprise Plan: Long-Term Climate Variability. It shows that the 18-year trends in Antarctic sea ice cover growth and Arctic decay may be portions of a 30 or more year cycle.

Modal Behavior of Hemispheric Sea Ice Covers

Per Gloersen and Norden Huang

Oceans and Ice Branch, Laboratory for Hydrospheric Processes

NASA/Goddard Space Flight Center

Greenbelt, Maryland 20117

Zheng Shen

Division of Engineering Science

California Institute of Technology

Pasadena, California 91125

Submitted to *JGR Oceans*

8.20.98

Abstract: Recent papers have described 18-year trends and annual oscillations in the Arctic and Antarctic sea ice extents, areas, and enclosed open water areas based on a newly-formulated 18.2-year ice concentration time series. This time series includes data for the entire Arctic and Antarctic ice covers, as well as for previously defined subregions consisting of 5 sectors in the Antarctic and 9 regions in the Arctic. It was obtained by fine-tuning the sea ice algorithm tie points individually for each of the four sensors used to acquire the data. In this paper, we extend these analyses to an examination of the intrinsic modes of these time series, obtained by means of Empirical Mode Decomposition, with emphasis on periodicities greater than the annual cycle. Quasibiennial and quasiquadrennial oscillations observed with a different technique and reported earlier for the first 8.8 years of this time series were also observed in the present series. However, the intrinsic modes were not monochromatic; they feature frequency as well as amplitude modulation within their respective frequency bands. Modal periods of up to 18 years are observed, with important implications for the trend analyses published earlier. These results are compared with the oscillations in the Length-of-Day and North Atlantic Oscillation parameters similarly determined for the same 18.2-year period.

Introduction:

The amount of sea ice in the hemispheric canopies has frequently been described as an indicator of climate change [e.g., Kellogg, 1975]. In order to assess recent climate changes, a seamless 18.2-year data set of sea ice concentrations over the time span of 1978-1996 has been recently produced [Cavalieri et al., 1997, 1998]. The observations were made with four different instruments, the Scanning Multichannel Microwave Radiometer (SMMR) on board the NASA Nimbus 7 satellite and three Special Sensor Microwave/Imagers (SSMIs) onboard the F8, F11, and F13 Defense Meteorological Satellite Program orbiters. In order to discern short-term climate changes, Parkinson et al. [1998] used these data to determine overall and seasonal trends for the Arctic sea ice canopy as a whole and for its subregions, as defined earlier [Gloersen et al., 1992]. Zwally et al. [1998] undertook a similar analysis for the Antarctic. Gloersen et al. [1998] analyzed the spatial distribution of the trends in these data and of the seasonality in the ice packs for both hemispheres. The trends were determined in two different ways: (1) An ordinary least squares, multiple linear regression method was used in which the intercept, slope, and coefficients for five harmonics of the annual cycle (12 coefficients in all) were determined simultaneously [Gloersen and Campbell, 1991a]. (2) A band-limited regression (BLR) method was used in which the data are filtered with a multiple-window bandpass filter that eliminates oscillations with periods shorter than 1/4 of the data span [Gloersen and Campbell, 1991b]. The reported BLR trends all have statistical confidence levels of 99% or better, but could also be affected by long-term oscillations with periods of 4.5

years or greater. Gloersen [1995; ...et al., 1996; ... and Mernicky,1998] observed quasiquadrennial oscillations in shorter time series consisting solely of SMMR data using a spectral analysis technique that included multiple-window filtering [Thompson, 1982; Lindberg, 1986; Park et al., 1987; Lindberg and Park, 1987; Kuo et al., 1990]. While not conclusive because of the brevity of the time-series, there was also an indication of longer-period oscillations in these earlier data.

In this paper, we extend the earlier spectral analyses to the combined SMMR/SSMI data set, but we depart from the earlier techniques. Instead we utilize an Empirical Mode Decomposition (EMD) recently developed by Huang et al. [1997], followed by the calculation of instantaneous periodicities through the use of an Hilbert transform, as described later. We also compare the ice canopy oscillations with those in the Length-of-Day (LOD) [Dickey et al., 1992, 1993] and North Atlantic Oscillation (NAO) parameters in the same time interval.

Empirical Mode Decomposition:

We shall utilize the EMD method developed by one of us [Huang et al., 1997] to analyze the oscillatory behavior of the hemispheric ice covers during the time span of 1978-1996. A simplistic outline of this method of sifting a data vector, y(n), into nearly orthogonal components is expressed as the following stepwise procedure:

1. Obtain two vectors containing the extrema of y(n).

2. Fit maxima and minima with two cubic spline vectors of length n.

3. $m_1(n)$ = average of the two cubic spline vectors.

4. First component, $c_1 = y(n) - m_1(n)$.

5. Repeat steps 1 - 3 on $m_1(n)$ to obtain $m_2(n)$.

6. Second component, $c_2 = m_1(n) - m_2(n)$.

...

i. ith component, $c_i = m_{i-1}(n) - m_i(n)$.

Continue until c_i contains less than one whole oscillation.

Usually converges for i = 8 to 10.

The actual method is more complicated than this in that there are conditional tests for how many time series points are allowed between the extrema of the various modes, or how many are allowed between the extrema of the curvatures of the modes. The selection of these criteria is subjective and the modes are not unique. On the other hand, if the criteria are judiciously selected, the resultant modes are nearly orthogonal. A benefit of this approach is that the oscillations in the various modes are confined to narrow frequency bands, greatly simplifying the interpretation of the results. Another benefit is that the original signal (within machine accuracy) is regained when the modes are added back together, an indication that spurious signals have not been introduced as a result of the decomposition.

After decomposition, the resulting intrinsic modes are further analyzed by producing a spectrum of their time-dependent periodicities by differentiating their Hilbert transform phases. We shall refer to this procedure as producing the Hilbert spectrum.

Details of the Oscillations in Arctic Sea Ice Extents:

We first apply the EMD method to the time series of Arctic sea ice extents, the sum of all Arctic sea ice grid areas with ice concentrations greater than 15%. With the decomposition parameters selected, eight intrinsic modes result, as shown in Figure 1. The first three modes (c1, c2, and c3 in Figure 1) have periods shorter than two months, and are not of interest for the bulk of this paper. Modes 2 and 3 appear occasionally to have some common periodicities that could probably be reassigned by more meticulous sifting in the decomposition process if we were to analyze them, but we have postponed that until such time as the shorter periodicities deserve our attention. Except for the sharp spike late in 1984, from an unknown source, the amplitude of the signal in the first mode is the lowest of all, being about two orders of magnitude below the seasonal cycle (mode 4). The "hash" level in this mode represents real day-to-day fluctuations in the sea ice resulting from atmospheric interactions. The "hash" components in modes 3 and 4, with periodicities of 1-7 weeks, are slightly larger, but the periodicities of 1-2 months found in both modes, probably attributable to tidal oscillations [Gloersen and Huang. 1998] are only an order of magnitude lower than the seasonal cycle, and comparable to modes 5-8. To demonstrate the efficacy of this procedure, we superimpose a plot of the recombination of modes 4-8 on a plot of the original data, with the seasonal cycle mode removed, in Figure 2. If we were to recombine all of the modes for this superposition and plot the combination on top of the original data, then the two curves would be indistinguishable.

We have referred to Mode 4 as the seasonal rather than annual cycle because it is clearly not a pure sinusoid with a 1-year period. In this respect, it is similar to a modeled seasonal cycle described in earlier papers [e.g., Gloersen et al., 1992]. The modeled seasonal cycle consists of a Fourier series of five harmonics (ten components) of the annual cycle. Mode 4 differs from the model, which has the same shape each year, in that there are some year-to-year differences in its shape. Examination of the Hilbert spectrum of the observed seasonal cycle (Figure 3) reveals another difference in the modeled and observed results. Ignoring the startup and closing transients caused by the smoothing function applied to the Hilbert transform phase before differentiating to obtain the periodicity, there is no evidence of the higher harmonics of the annual cycle used in the model in the observed seasonal cycle. In fact, the shortest period encountered in the observed seasonal cycle is about 0.6 years. It is clear that the seasonal cycle is frequency modulated within the annual time span and that the FM pattern is not identical from one year to the next.

We shall refer to mode 5 (c5 in Figure 1) as the quasibiennial mode because its period usually appears to be about 2 years. Its Hilbert spectrum (Figure 3) shows that it, too, is frequency modulated, reaching periods as long as four years late in 1982. (The digression to very long periods in 1991, arithmetically cut off at 12 years to keep the scale below that, results from the nearly flat modal amplitude (Figure 1) at that time.) The multiple-window filtered Fourier spectrum [Thompson, 1982; Lindberg, 1986; Lindberg and Park, 1987; Park et al., 1987a, 1987b; Kuo et al., 1990] of the recombination of modes 5-7 (Figure 4) shows a series of peaks near the 2-year period rather than the single quasibiennial peak obtained from the raw ice extent data and reported earlier [Gloersen, 1995]. In view of the complicated frequency modulation in mode 5 (Figure 3), it is not clear that this multipeaked structure (Figure 4) has any physical significance. However, the asymmetrical shape of the biennial peak observed earlier can now be explained on the basis of the frequency modulation of mode 5.

A similar narrative can be applied to the quasiquadrennial (QQ, c6) and quasioctennial (QO, c7) modes shown in Figure 1 and their multiple-window filtered Fourier spectra in Figure 3. It is apparent in Figure 4 that the Fourier spectrum of what we have called the QQ mode also contains some of the QO oscillation. Again, the multiple peak characteristic of this spectrum probably has no useful significance, but is more likely a meaningless consequence of the FM structure in that mode. The quasioctennial peak was not shown earlier by Gloersen [1995] because the time series spanned only the first nine years of the one discussed here.

Although Mode 8 (Figure 1) could be interpreted as an oscillation with a period of about 33 years, there are clearly not enough data to apply this description with any reasonable degree of certainty. Mode 8 appears to be the major contributor to the negative trend in Arctic sea ice extent reported earlier [Gloersen and Campbell, 1992; Cavalieri et al., 1997; Parkinson et al., 1998]. The increase in the negative trend in the latter half of this time span reported by these authors is nicely explained by the modal pattern. If mode 8 truly is a 33-year oscillation, then there will be a trend reversal in the Arctic sea ice extents over the next 16 years.

Interannual Oscillations in the Overall Arctic and Antarctic Sea Ice Area, Extent, and Enclosed Open Water Areas:

In the remainder of this paper, we shall confine our discussion to the modes containing periods of greater than one year. We shall also make our comparisons one mode at a time. Since the various modes are generally strongly frequency-modulated, attributing the labels quasibiennual (QB), quasiquadrennial (QQ), and quasioctennial (QO) to some of them is somewhat arbitrary, but we choose to label them so in accordance with the predominant period in their oscillations. More precisely, they are named in sequence in the successive modes of increasing periodicity after the seasonal cycle mode.

It is interesting also to investigate the sea ice area, the sum of the concentration-weighted areas of the grid map pixels, and the open water area within the pack, the difference between the sea ice extent and area. The QB modes of these attributes are shown in Figure 5. In this figure, the ordinate labels AR_ and AA_ signify Arctic and Antarctic, respectively, and _X, _A, and _OW signify sea ice extent, area, and enclosed open water, respectively. There is no obvious correlation between the QB oscillations in the sea ice covers or the enclosed areas of open water of the Arctic and Antarctic. Indeed, the average periods of these QB oscillations differ for the north and south, and so they slip in and out of phase during this 18-year time interval. Therefore, we are led to believe that these oscillations must be related to local resonances and/or driving forces, and are likely sums of such interactions on an even more local basis.

The extent and area QB modes of each hemisphere do bear some resemblance to each other, but are sufficiently dissimilar so as to result in net oscillations in the amount of open water in the pack, with comparable amplitudes. Note, however, that the _OW curves in Figure 5 are not simply the difference of the _X and _A curves but are obtained from an independent EMD applied to the open water time series. The similarity of the QB modes of the extent and area series of each hemisphere implies that these oscillations are typical of the entire pack and not just the marginal ice. This may exclude ocean-ice boundary interactions and favor interactions between the ice and the atmosphere as the source of the oscillations. The cause of the amplitude modulation in these modes in not presently understood, but it should be realized that this modulation is not an expression of longer-period modes, since the EMD process also extracts those.

The QQ modes of the Arctic ice areas and shown in Figure 6 are one of the two most regular, with the periods varying between about 4.5 - 5.5 years. The Arctic extent follows the area during 1991-1997 and the peaks also coincide in 1983, but otherwise the oscillation in the extent and the area bear little resemblance. The QQ mode in the enclosed open water areas of the Arctic are also quite regular, but with periods quite different from the area and extent, ranging from 3.5 to 4.2 years.

In the Antarctic, the QQ mode in the ice extent (Figure 6) does not develop well-defined oscillations until 1984, when a 2.5- 4.3-year oscillation starts building to maximum amplitude in 1995. The QQ mode in the area on the other hand is better defined in the earlier half of the time interval, with periods near 3.7 years. Curiously, the QQ mode in the Antarctic open water areas is more regular and matches the open water signal in the Arctic, with the exception of 1995-7.

The QO modes designation for the oscillations shown in Figure 7 truly stretch the validity in the terminology, although, keep in mind, we have arbitrarily defined the QB, QQ, and QO modes as those modes of increasing periods starting from the seasonal cycle. The QO mode for the Arctic sea ice extent shown in Figure 7 as ARX is shown also in Figure 1 as Mod7. Its regularity served as one of the inspirations for the QO designation. The observed periods are as short as 4.5 years for the mid portion of the Antarctic sea ice extent and as long as 10 years for the Arctic sea ice area. The QO mode in the Arctic sea ice area (ARA in Figure 7) may be a combination of two oscillations, one with a 10-year period, and the other a very long period similar to that of the Arctic sea ice extent shown as Mod8 in Figure 1. A trend line fitted through ARA would have very similar characteristics to those reported earlier for the monthly anomalies [Cavalieri et al., 1997]. Again, the lack of any obvious correlation between the QO modes of these various components is suggestive of localized interactions, or even more likely, sums of localized interactions.

Interannual Oscillations in the Subregions of the Arctic and Antarctic:

Earlier studies have indicated different spectral signatures for the ice areas and extents in the various subregions of each hemisphere [Gloersen, 1995]. Here, then, we examine the modal structure of 9 regions in the Arctic and 5 sectors in the Antarctic as defined elsewhere [Gloersen et al., 1992] in a search for similar differences. We shall restrict ourselves to description of the sea ice areas since this quantity is the most representative of the subregional properties.

The QB oscillations in the 9 Arctic regions are shown in Figure 8, with also the total Arctic sea ice area shown for comparison. After 1981, the total Arctic and the region called the Arctic Ocean (ArOc) have fairly similar oscillatory structures, with periods ranging from 1.5 to 2 years. This similarity is to be expected, since the Arctic Ocean signal represents a large part of the total. Part of the ArOc signal, from 1986 to 1993 appears at first to be repeated with a lag of about 2.5 years in the Canadian Archipelago (Carc in Figure 8), but since the rest of the patterns do not match we believe this apparent partial match to be fortuitous. A similar probably fortuitous match of this signal appears in Baffin Bay in about the same time period.

There is also little correlation between QB modes of the seas opening to the North Pacific, the Bering Sea, and the Seas of Japan and Okhotsk (Brng and O/J in Figure 8). This is not unexpected, in view of earlier observations of dependencies on localized weather patterns such as a shifting Aleutian Low [Cavalieri and Parkinson, 1987]. For the seas opening to the North Atlantic, the St. Lawrence, Baffin Bay, the Greenland, and the Kara/Barents, there is again little correlation and the indication of local dependencies.

In the so-called QO modes shown in Figure 10 for the Arctic regions, the periods range from about 5 years for the well-developed oscillation in the Arctic Ocean to what might be construed as a 14-year oscillation in the Kara/Barents Seas. This adds credence to the idea that the various regions are not being driven by a common source.

One might expect to see more correlation between the Antarctic sea ice areas in the adjacent sectors since except for the Antarctic Peninsula they are connected, and since the perimeter is in contact with the Antarctic Circumpolar Current and large-scale atmospheric features like the Antarctic Trough. However, examination of the QB, QQ, and QO modes (Figures 11-13) does not support this expectation. The lack of inter-sector coherence in any of these modes is just as apparent as it is in the Arctic regions. The QQ designation for the Indian Ocean sector (Indn in Figure 12) is clearly a misnomer, but it is the second mode after the seasonal cycle and also the last mode decomposed by EMD. Hence that sector is not displayed in Figure 13 in the QO modes.

We conclude after analyzing all of this that there is little evidence presented for coherence in the hemispheric sea ice cover oscillations. The results also imply that coherency in the oscillations are probably on smaller scales and in differently-shaped regions and sectors as observed earlier [Gloersen et al., 1996; Gloersen and Mernicky, 1997] with the use of spectral analysis of multiple-window filtered data on a single-pixel basis. While it is a daunting prospect, we are developing a procedure for applying EMD to the single-pixels of hemispheric ice concentration grid maps, which we expect to report in subsequent papers.

Comparison of the Intrinsic Modes of the North Atlantic Oscillation, the Southern Oscillation Index, the Length-of-Day Parameter, and the Global Total of the Hemispheric Ice Covers:

We have chosen to combine the hemispheric sea ice areas, extents, and enclosed water amounts into their respective global sums for the purpose of comparison with another global parameter, the rotational rate of the earth, as expressed in the Length-of-Day parameter (LOD) described elsewhere [Dickey et al., 1992; 1993]. Based on earlier data, including the early part of this time series, Dickey and others have suggested the use of the LOD parameter as a proxy for the Southern Oscillation Index (SOI) and the zonal average angular momentum (AAM) of the earth's atmosphere. Others [?? Ref] have suggested a connection between the variations in the Arctic sea ice cover, at least that portion connected to the North Atlantic and the variations in the North Atlantic Oscillation (NOA). For these reasons, we have provided the QB, QQ, and QO intrinsic modes of these parameters in Figures 14-16, along with those modes of the global sums of the sea ice cover parameters.

The notion of using LOD as a proxy for SOI seems to be valid up through 1984 in the QB and QQ modes, but not after that, or at all for the QO modes. The QB modes for the three global sea ice parameters all seem to be in a narrow band around about 1.9 years. The QB modes for LOD, on the other hand, are not as narrow band and have periods of 2.2 years or longer. The NOA QB mode, at least, oscillates with period as short as 1.9 years early in this record, but the period of this mode increases to 3 years later in the record. The periodicities in the SOI QB mode range from 1.5 to 2.2 years.

In the QQ modes (Figure 15), the only correlation, probably fortuitous, observed is between the NOA and the global sea ice extent (GlbEx in Figure 15), and then only until 1991 after which the signals are no longer in phase. Another probably fortuitous correlation is between the QO modes (Figure 16) of the SOI and the global open water amount (GlbOW in Figure 16), where the GlbOW leads the SOI by about 2-3 years.

These observations force us to conclude that as far as interdecadal oscillations are concerned, there appear to be no significant correlations between the LOD, SOI, and NOA parameters, and the global or hemispheric sea ice parameters.

References:

Cavalieri, D. J., and C. L. Parkinson, On the relationship between atmospheric circulation and the fluctuations in the sea ice extents of the Bering and Okhotsk Seas, *J. Geophys. Res.* **92**, 7141-7162, 1987.

Cavalieri, D. J., Gloersen, P., Parkinson, C. L., Comiso, J.C., and Zwally, H.J., Observed asymmetry in global sea ice changes, 1997, *Science* **278**, 1104-1106.

Cavalieri, D. J., C. L. Parkinson, P. Gloersen, J. C. Comiso, and H. J. Zwally, Deriving Long-term Time Series From Satellite Passive Microwave Multisensor Data Sets, J. Geophys. Res., *submitted*, 1998.

Dickey, J. O., S. L. Marcus, and R. Hide, Global propagation of interannual fluctuations in atmospheric angular momentum, *Nature, 357*, 484-488, 1992.

Dickey, J. O., S. L. Marcus, T. M. Eubanks, and R. Hide, Climate studies via space geodesy: Relationships between ENSO and interannual length-of-day variation, *in Interaction Between Global Climate Subsystems, Geophysical Monograph. Ser.*, vol. 75, edited by G. A. McBean and M. Hantel, pp. 141-155, AGU, Washington, D.C., 1993.

Gloersen, P., and W. J. Campbell, Variations of extent, area, and open water of the polar sea ice covers: 1978-1987, in *Proceedings of the International Conference on the Role of the Polar Regions in Global Change,* edited by G. Weller, C. L. Wilson, and B. A.. B. Severin, 778 pp., Geoph. Inst., Univ. of Fairbanks, Fairbanks, Alaska, 1991a.

Gloersen, P., and W. J. Campbell, Recent variations in Arctic and Antarctic sea ice covers, *Nature, 352*, 33-36, 1991b.

Gloersen, P., W. J. Campbell, D. J. Cavalieri, J. C. Comiso, C. L. Parkinson, and H. J. Zwally, Arctic and Antarctic sea ice, 1978-1987: Satellite passive-microwave observations and analysis, *NASA SP-511*, Washington D.C. 1992).

Gloersen, P., ENSO frequency components in the global sea ice covers, *Nature, 373*, 503-506, 1995.

Gloersen, P., J. Yu, and E. Mollo-Christensen, Oscillatory behavior in Arctic sea ice concentrations, *J. Geophys. Res., 101*, 6641-6650, 1996.

Gloersen, P, and A. Mernicky, Oscillatory behavior in Antarctic sea ice concentrations, in *AGU Antarctic Research Series: Antarctic Sea Ice Physical Properties and Processes* **74**, M.O. Jeffries, ed., February 11, 1998.

Gloersen, P., C. L. Parkinson, D. J. Cavalieri, J. C. Comiso, and H. J. Zwally, Spatial Distribution of Trends and Seasonality in the Global Sea Ice Covers: 1978-1996, J. Geophys. Res., *submitted*, 1998.

Gloersen, P., and N. Huang, In search of an elusive Antarctic circumpolar wave in sea ice extents: 1978-1996, Polar Record, *submitted*, 1998.

Huang, N. E., Z. Shen, S. R. Long, M. C. Wu, H. H. Shih, Q. Zheng, N-C Yen, C. C. Tung, and H. H. Liu, The Empirical Mode Decomposition and the Hilbert spectrum for nonlinear and nonstationary time series analysis,. Proceedings of the Royal Society of London, Series A **454**, 903-995, 1998.

Kellogg, W. W., Climatic feedback mechanisms involving the polar regions, in *Climate of the Arctic,* G. Weller and S. A. Bowling, eds., Geophysical Institute, University of Alaska, pp. 111-116, 1975.

Kuo, C., C. R. Lindberg, and D. J. Thomson, Coherence established between atmospheric carbon dioxide and global temperature, *Nature, 343*, 709-714, 1990.

Lindberg, C. R., Multiple taper spectral analysis of terrestrial free oscillations, Ph.D. thesis, Univ. of Calif., San Diego, 1986.

Lindberg, C. R., and J. Park, Multiple-taper spectral analysis of terrestrial free oscillations, II, *Geophys. J. R. Astron. Soc.*, *91*, 795-836, 1987.

Park, J., C. R. Lindberg, and F. L. Vernon III, Multiple-taper spectral analysis of high-frequency seismograms, *J. Geophys. Res.*, *92*, 12,675-12,684, 1987a.

Park, J., C. R. Lindberg, and D. J. Thomson, Multiple-taper spectral analysis of terrestrial free oscillations, I, *Geophys. J. R. Astron. Soc. 91*, 755-794, 1987b.

Parkinson, C. L., D. J. Cavalieri, P. Gloersen, H. J. Zwally, and J. C. Comiso, Variability of Arctic Sea Ice 1978-1996, J. Geophys. Res., *submitted*, 1998.

Thomson, D. J., Spectrum estimation and harmonic analysis, *Proc. IEEE, 70,* 1055-1095, 1982.

Zwally, H. J., J. C. Comiso, C. L. Parkinson, D. J. Cavalieri, and P. Gloersen, Variability of Antarctic Sea Ice from Satellite Observations, J. Geophys. Res., *in manuscript*, 1998.

Figures:

Figure 1. Intrinsic modes of Arctic sea ice extents for October 26, 1978 - December 31, 1996.

Figure 2. A superposition of a recombination of modes 5-8 (heavy curve) on the original Arctic sea ice extent data, with the seasonal cycle (mode 4) removed, (dashed curve) for illustrative purposes.

Figure 3. Intrinsic modal spectrum of Arctic sea ice extents; modes 5-7 from Figure 1.

Figure 4. Multiple-window filtered Fourier spectrum of each of the intrinsic modes 5-7 of the Arctic sea ice extents from Figure 1.

Figure 5. Quasibiennial modes for Arctic and Antarctic sea ice extents, areas, and enclosed open water. The ordinate labels AR_ and AA_ signify Arctic and Antarctic, respectively, and _X, _A, and _OW signify sea ice extent, area, and enclosed open water, respectively. Units are 10^6 Km^2.

Figure 6. Quasiquadrennial modes for Arctic and Antarctic sea ice extents, areas, and enclosed open water.

Figure 7. Quasioctennial modes for Arctic and Antarctic sea ice extents, areas, and enclosed open water.

Figure 8. Quasibiennial modes for total Arctic sea ice areas, and for nine designated Arctic regions.

Figure 9. Quasiquadrennial modes for total Arctic sea ice areas, and for nine designated Arctic regions.

Figure 10. Quasioctennial modes for total Arctic sea ice areas, and for nine designated Arctic regions.

Figure 11. Quasibiennial modes for total Antarctic sea ice areas, and for five designated Antarctic regions.

Figure 12. Quasiquadrennial modes for total Antarctic sea ice areas, and for five designated Antarctic regions.

Figure 13. Quasioctennial modes for total Antarctic sea ice areas, and for five designated Antarctic regions.

Figure 14. Quasibiennial modes for the North Atlantic Oscillation, the Southern Oscillation index, and the length-of-day parameter, and for global sea ice extents, areas, and enclosed open water.

Figure 15. Quasiquadrennial modes for the North Atlantic Oscillation, the Southern Oscillation index, and the length-of-day parameter, and for global sea ice extents, areas, and enclosed open water.

Figure 16. Quasioctennial modes for the North Atlantic Oscillation, the Southern Oscillation index, and the length-of-day parameter, and for global sea ice extents, areas, and enclosed open water.

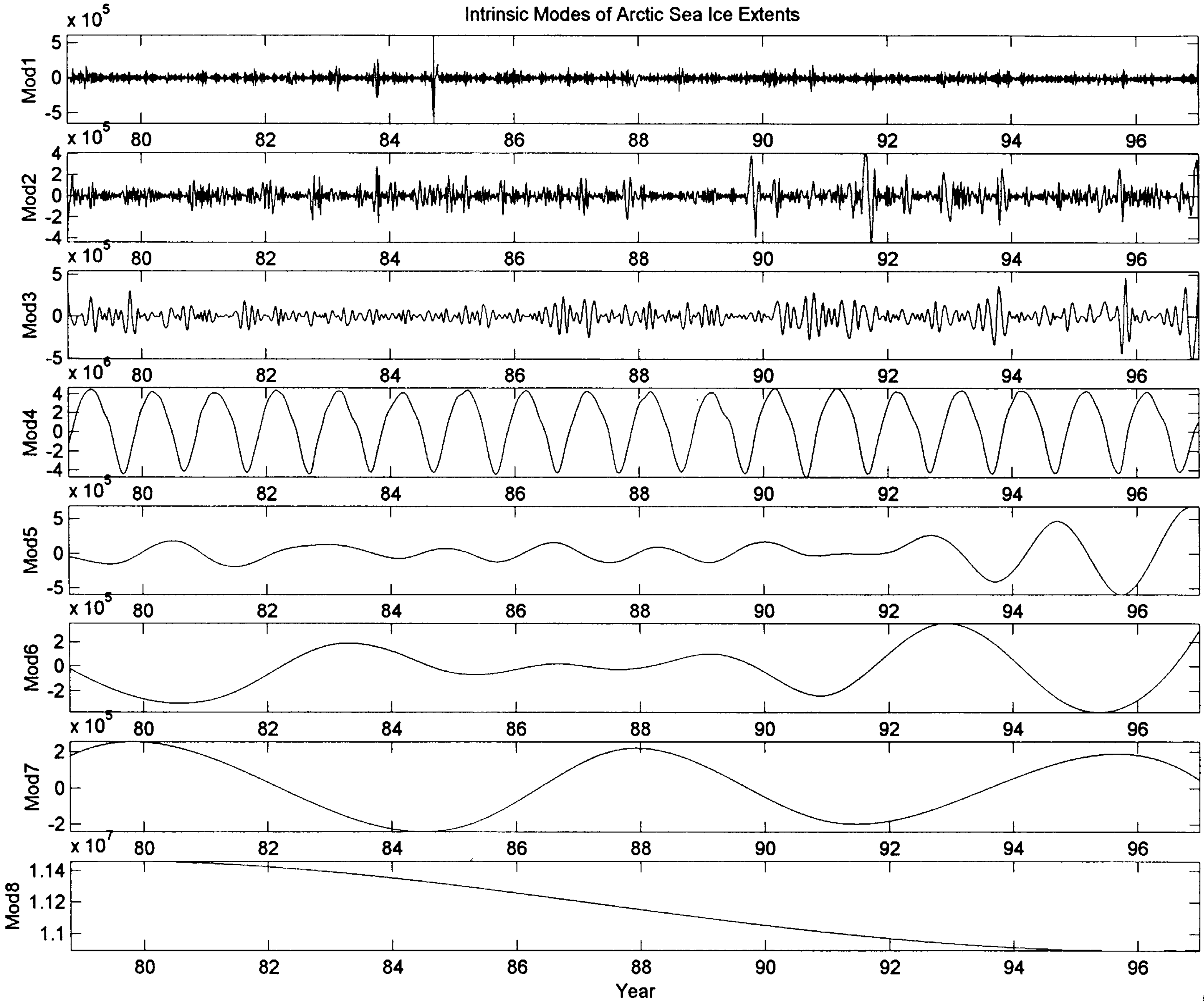
Intrinsic Modes of Arctic Sea Ice Extents
Mod1
Mod2
Mod3
Mod4
Mod5
Mod6
Mod7
Mod8
Year

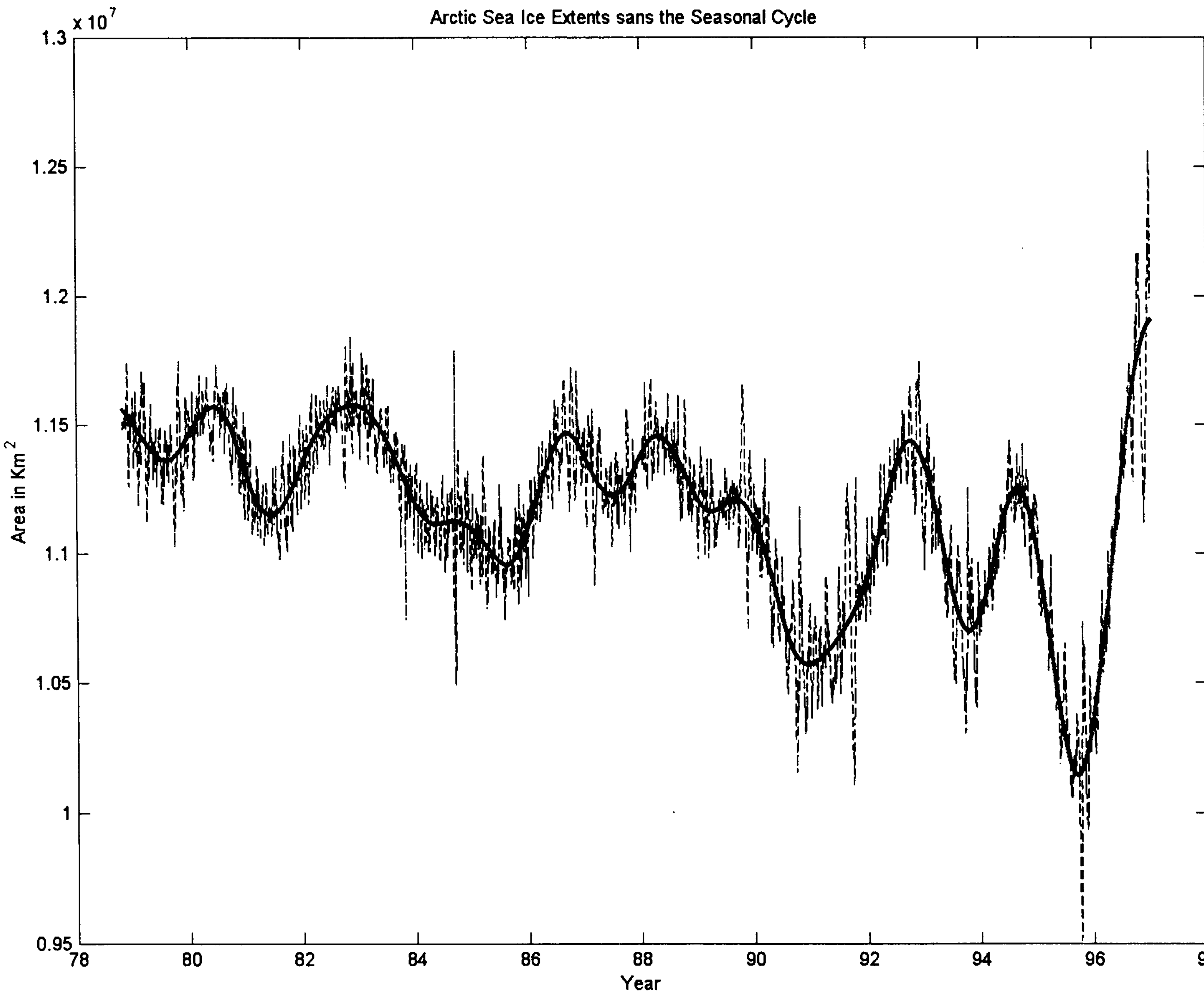
Arctic Sea Ice Extents sans the Seasonal Cycle
x 10^7
1.3
1.25
1.2
1.15
1.1
1.05
1
0.95
Area in Km 2
78
80
82
84
86
88
90
92
94
96
98
Year

2

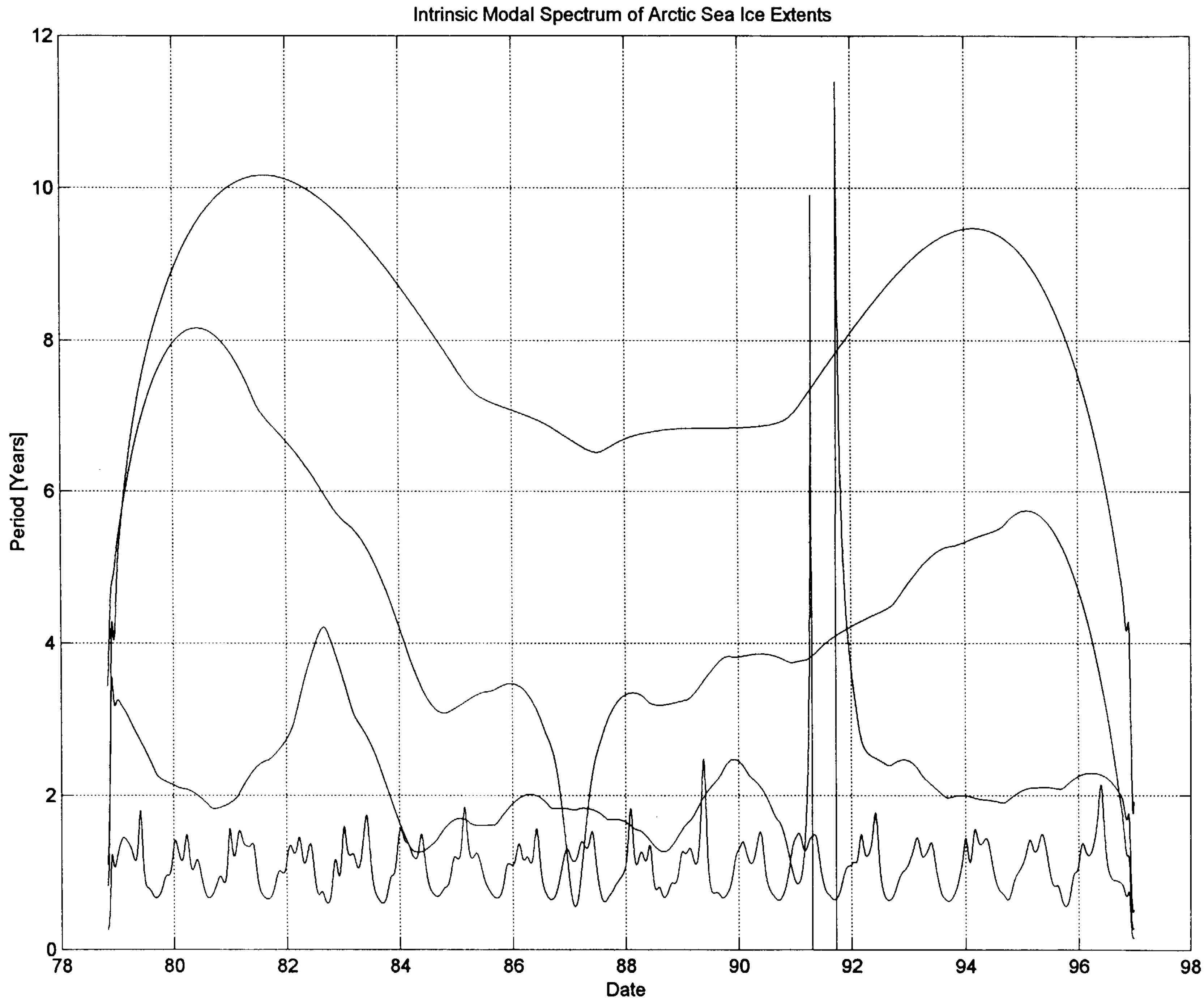
Intrinsic Modal Spectrum of Arctic Sea Ice Extents
Period [Years]
0
2
4
6
8
10
12
78
80
82
84
86
88
90
92
94
96
98
Date

3

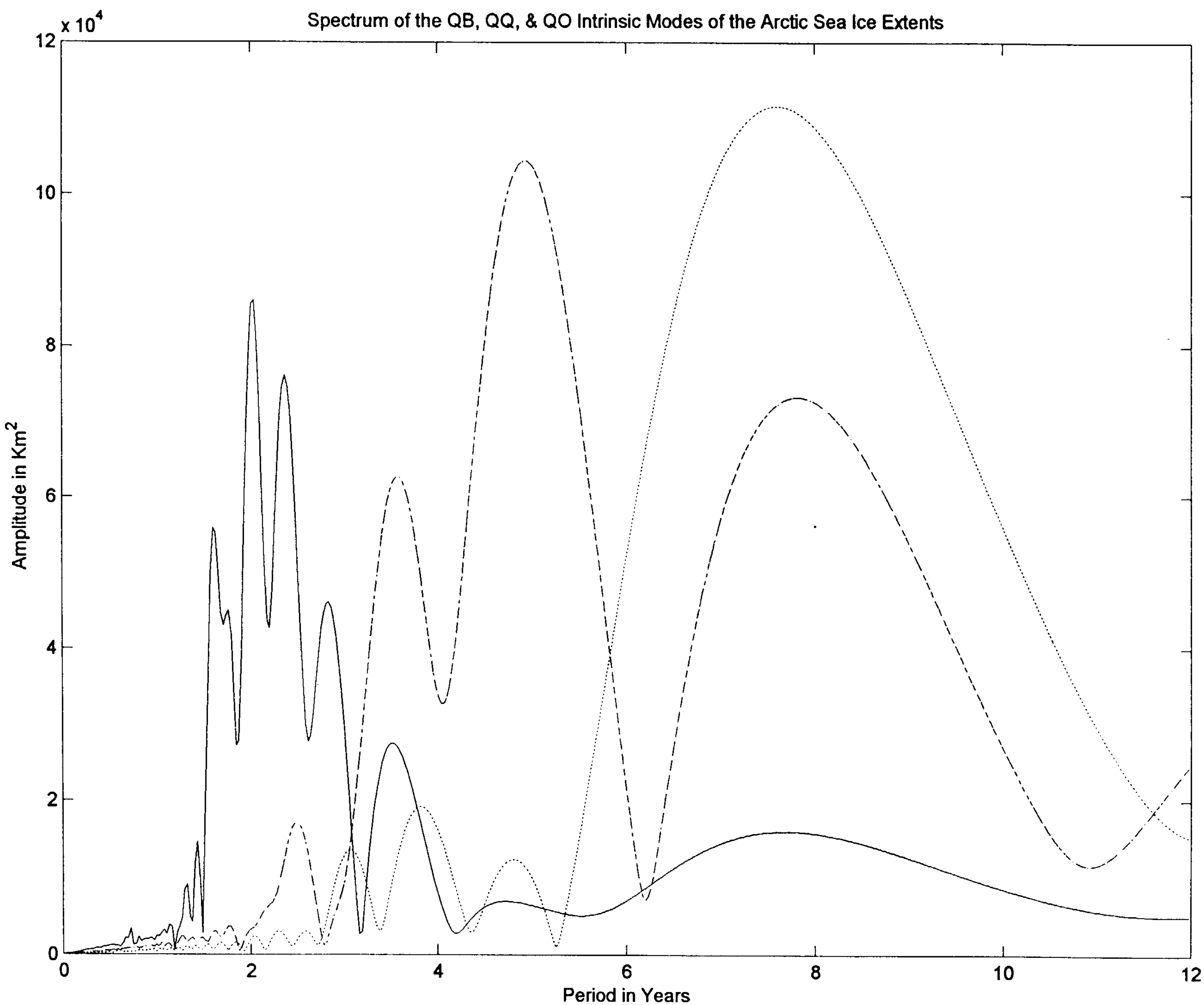

Spectrum of the QB, QQ, & QO Intrinsic Modes of the Arctic Sea Ice Extents
x 10^4
12
10
8
6
4
2
0
Amplitude in Km^2
0
2
4
6
8
10
12
Period in Years

4

Quasibiennial modes for Arctic and Antarctic Sea Ice Covers

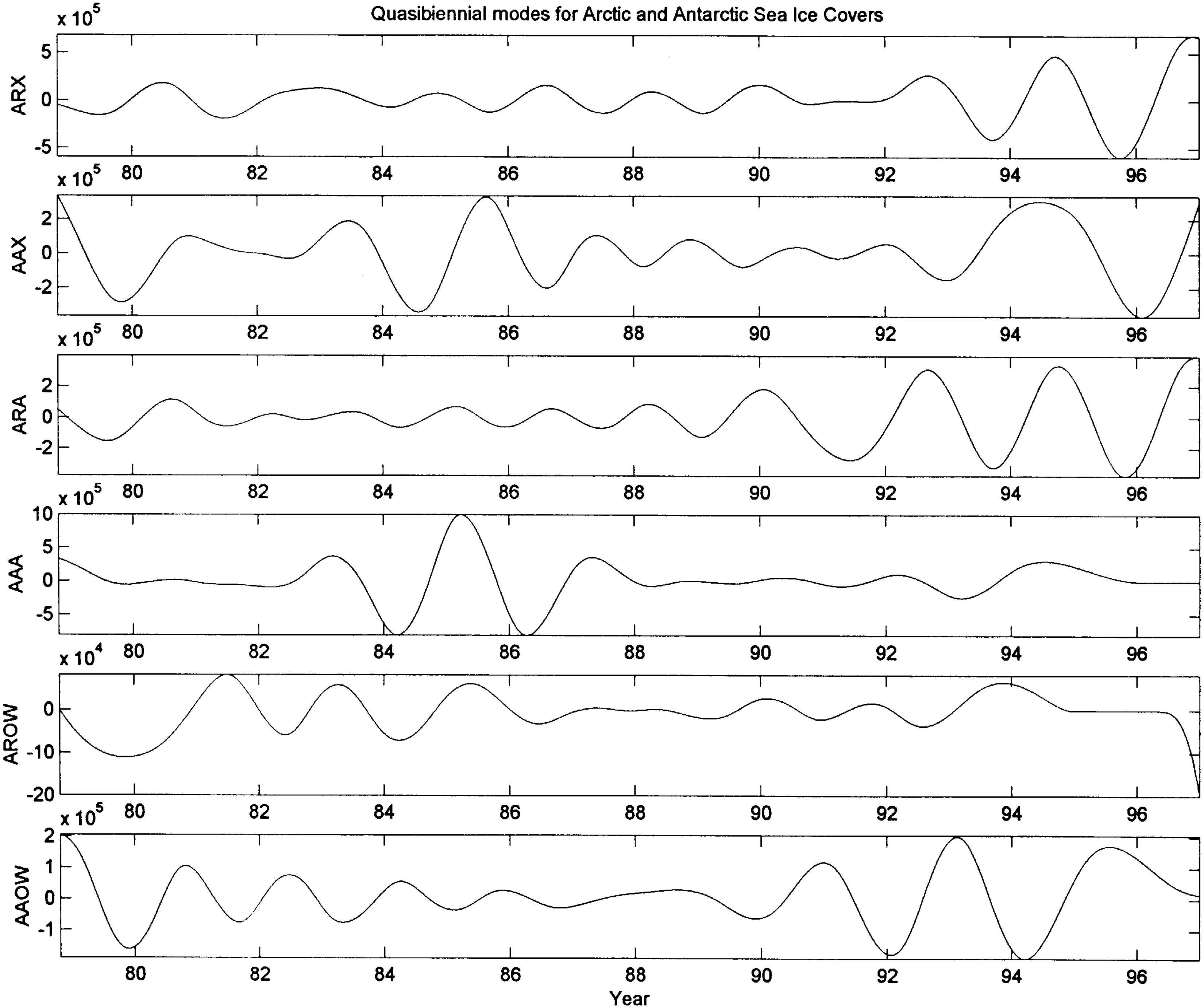

5

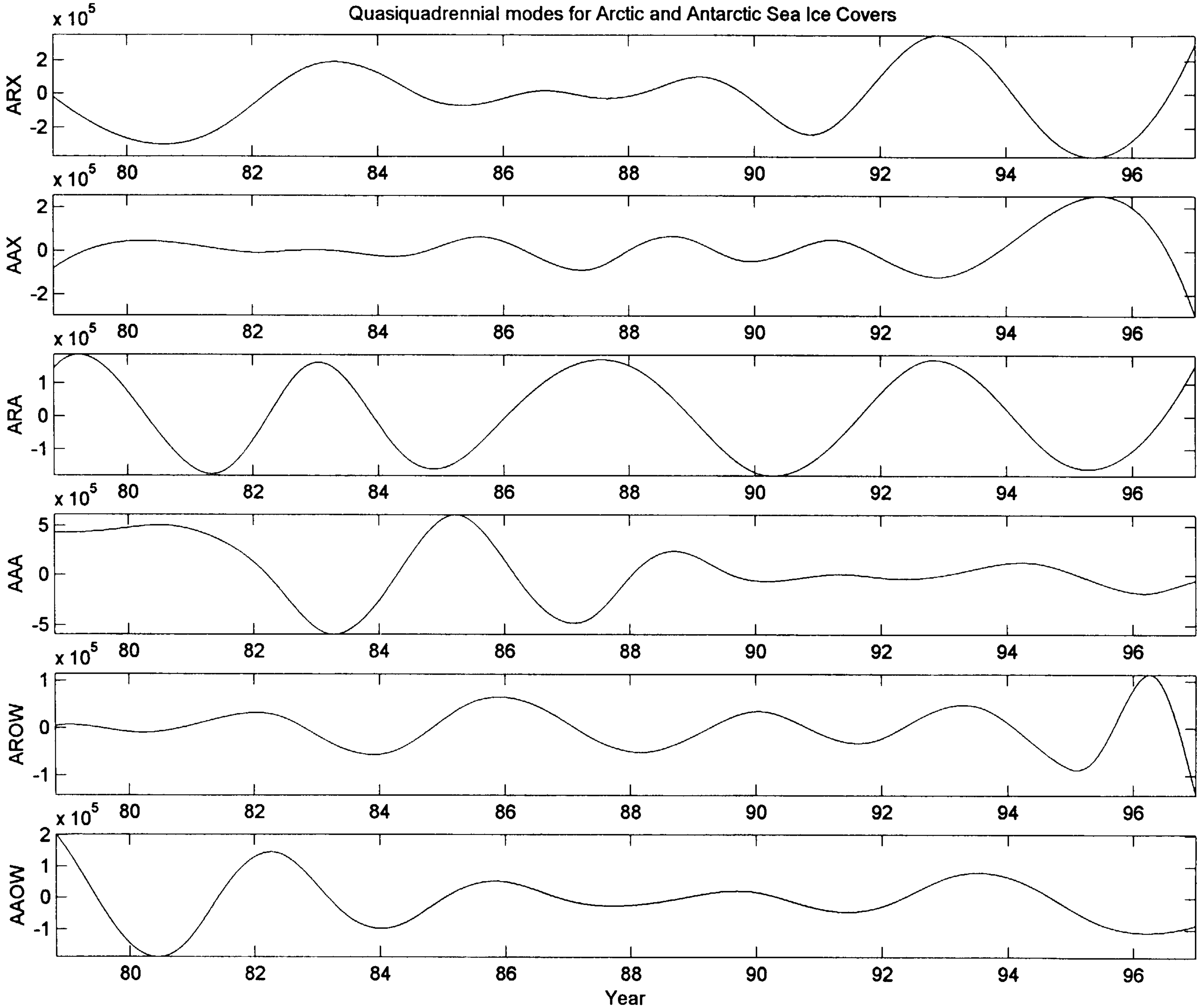

Quasiquadrennial modes for Arctic and Antarctic Sea Ice Covers
x 10^5
ARX
AAX
ARA
AAA
AROW
AAOW
80
82
84
86
88
90
92
94
96
Year

6

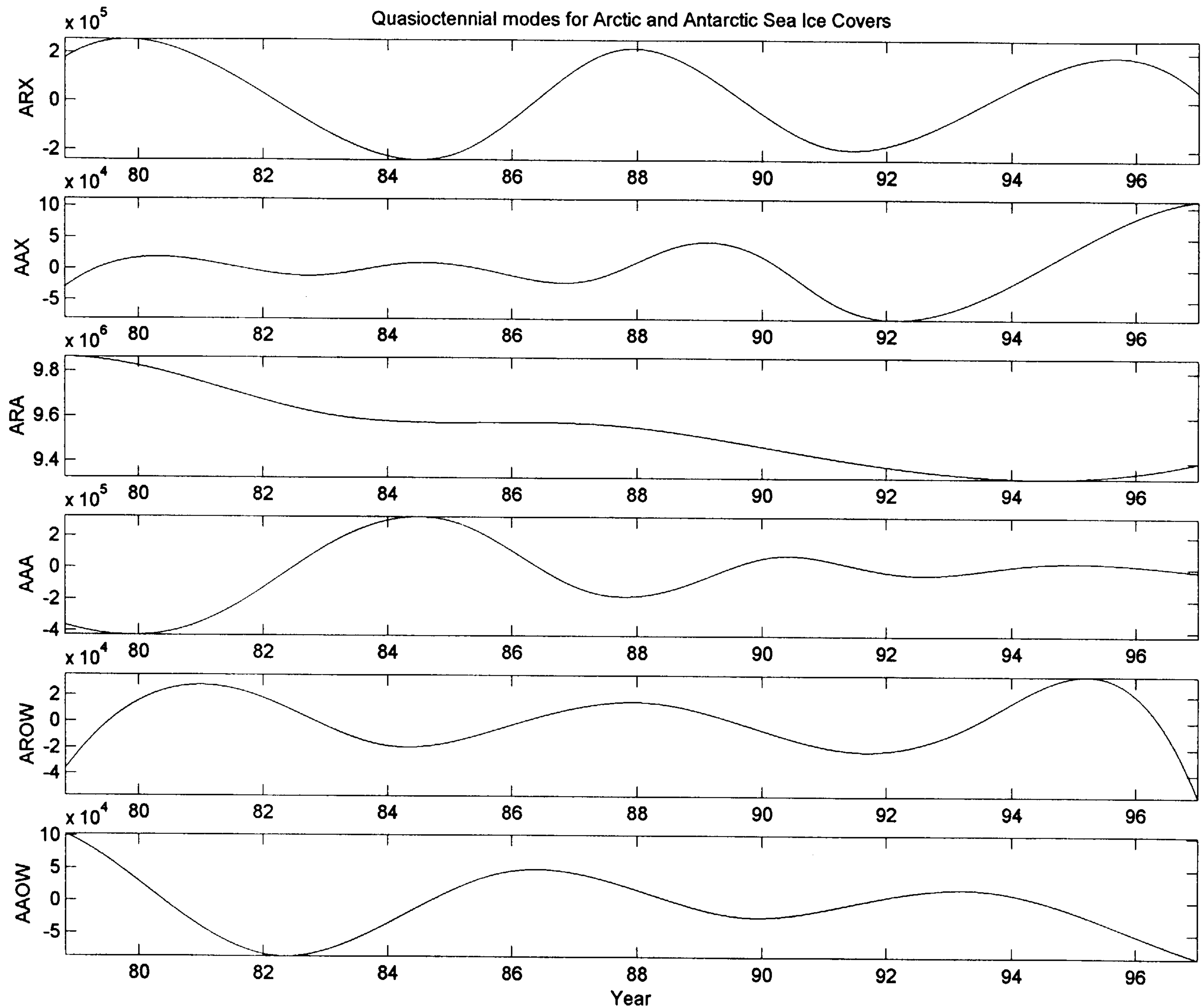
Quasioctennial modes for Arctic and Antarctic Sea Ice Covers
x 10^5
ARX
x 10^4
AAX
x 10^6
ARA
x 10^5
AAA
x 10^4
AROW
x 10^4
AAOW
80 82 84 86 88 90 92 94 96
Year

7

QB Modes for the Sea Ice Areas of the Arctic and Its 9 Regions

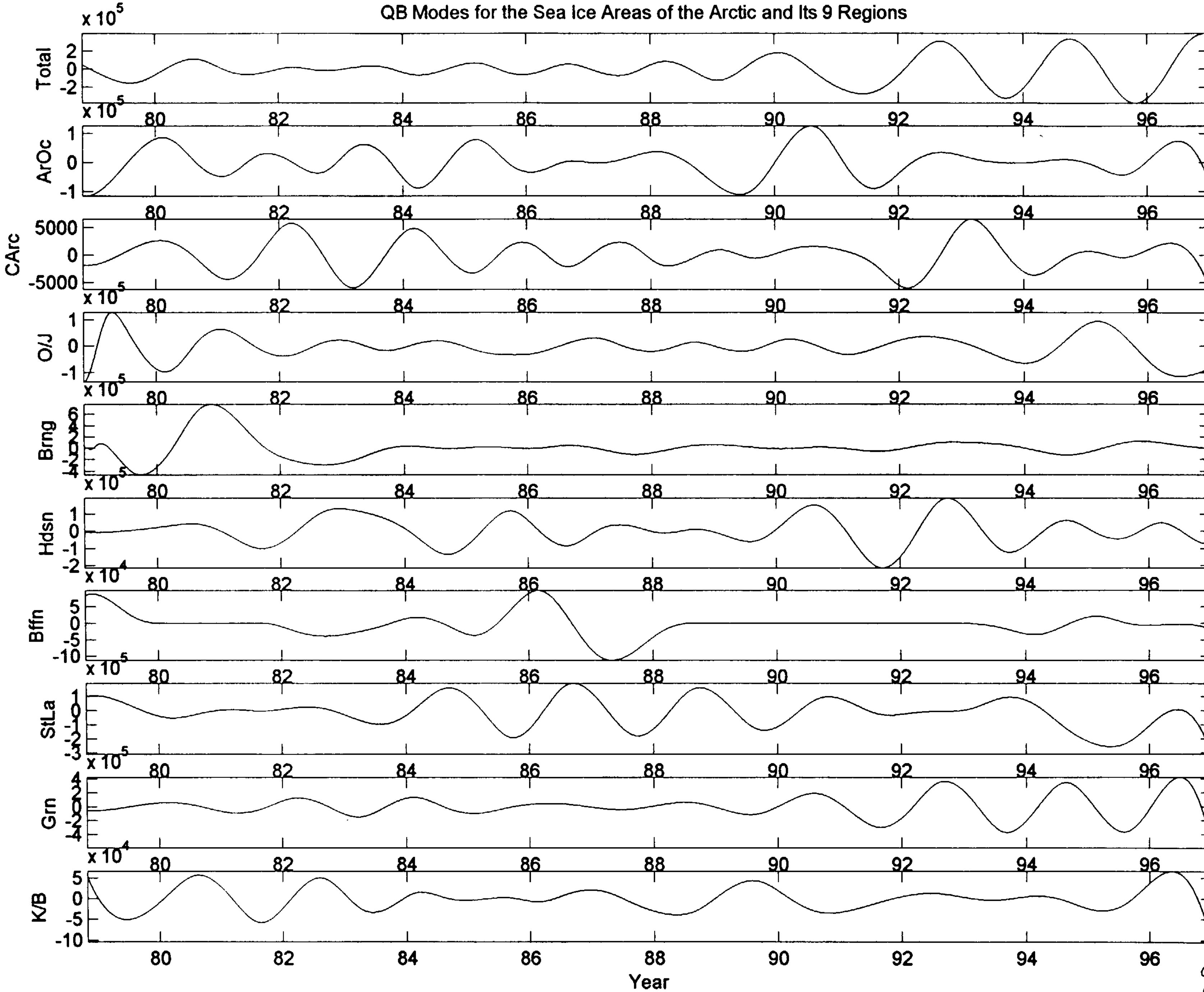

8

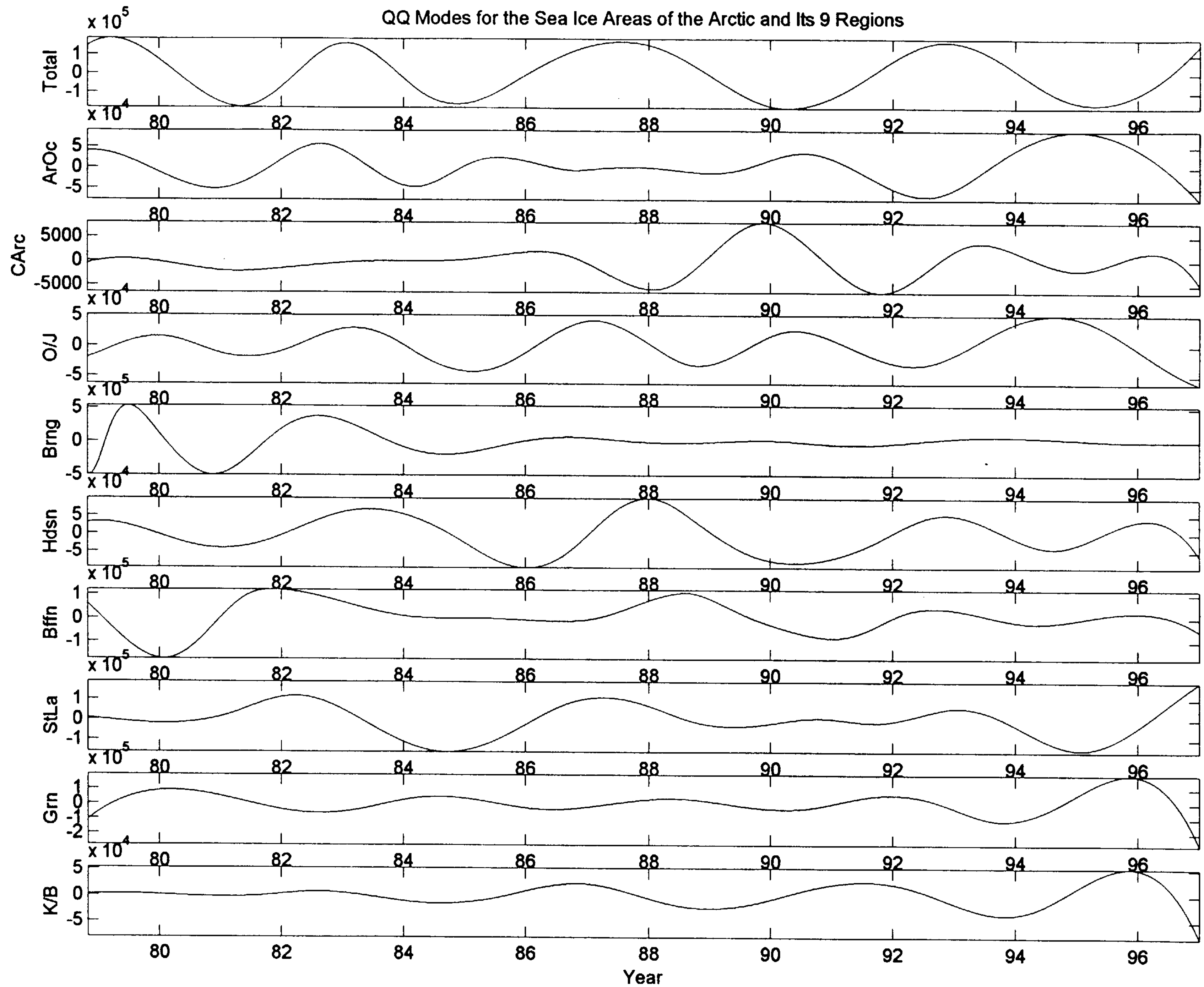
QQ Modes for the Sea Ice Areas of the Arctic and Its 9 Regions
Total
ArOc
CArc
O/J
Brng
Hdsn
Bffn
StLa
Grn
K/B
Year

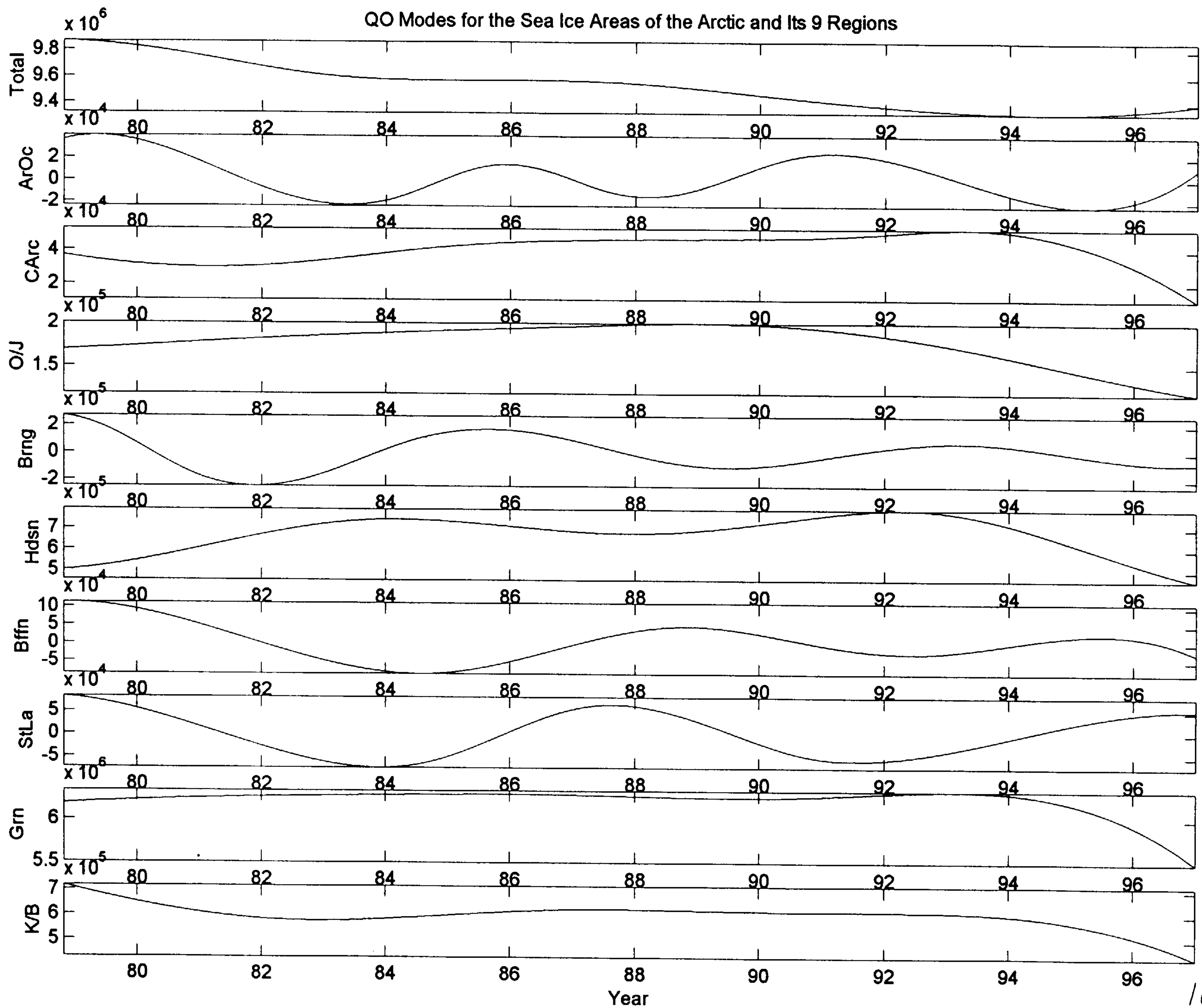

QO Modes for the Sea Ice Areas of the Arctic and Its 9 Regions
Total
ArOc
CArc
O/J
Brng
Hdsn
Bffn
StLa
Grn
K/B
Year

10

QB Modes for the Sea Ice Extents of the Antarctic and Its 5 Sectors

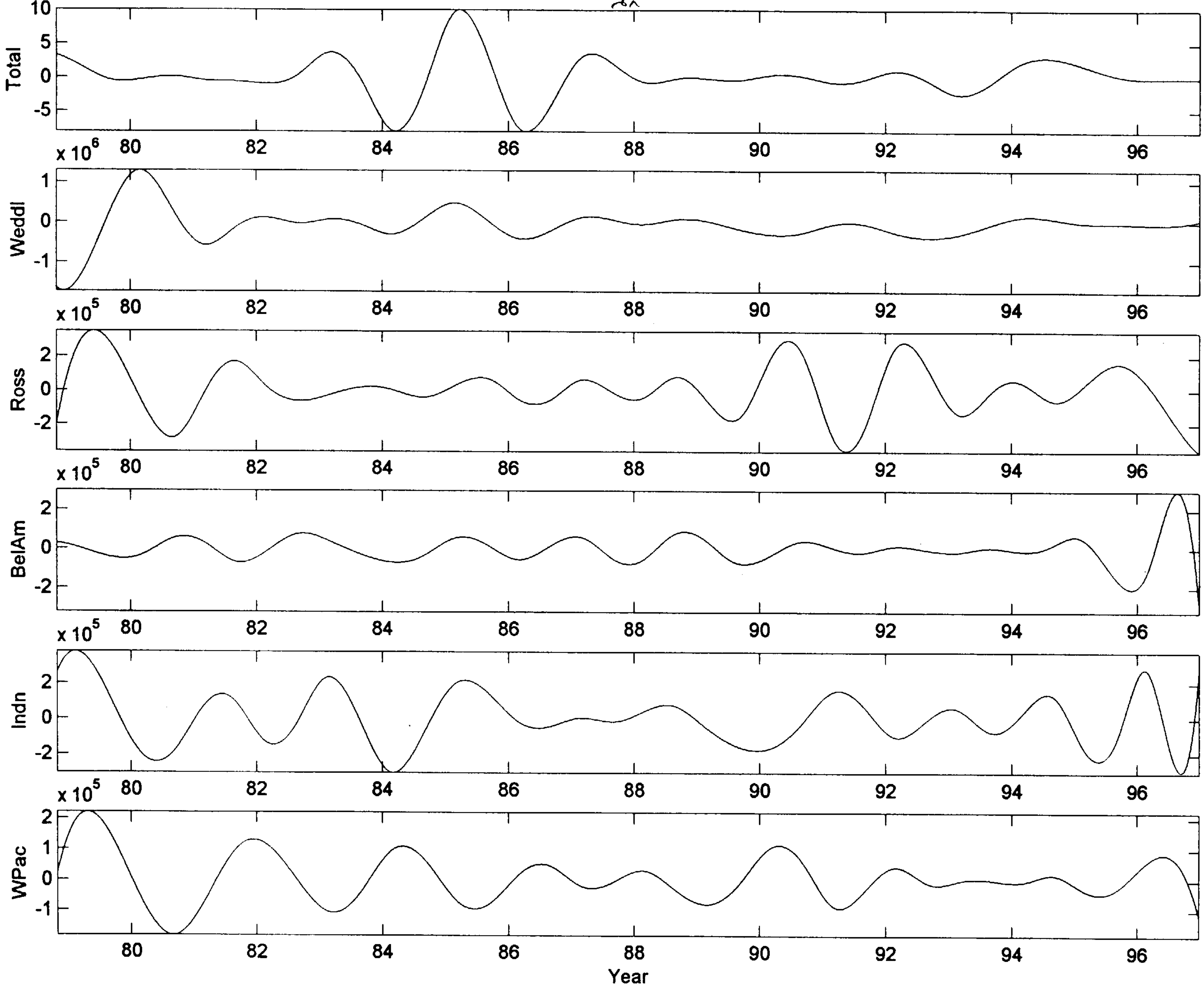

11

QQ Modes for the Sea Ice Extents of the Antarctic and Its 5 Sectors

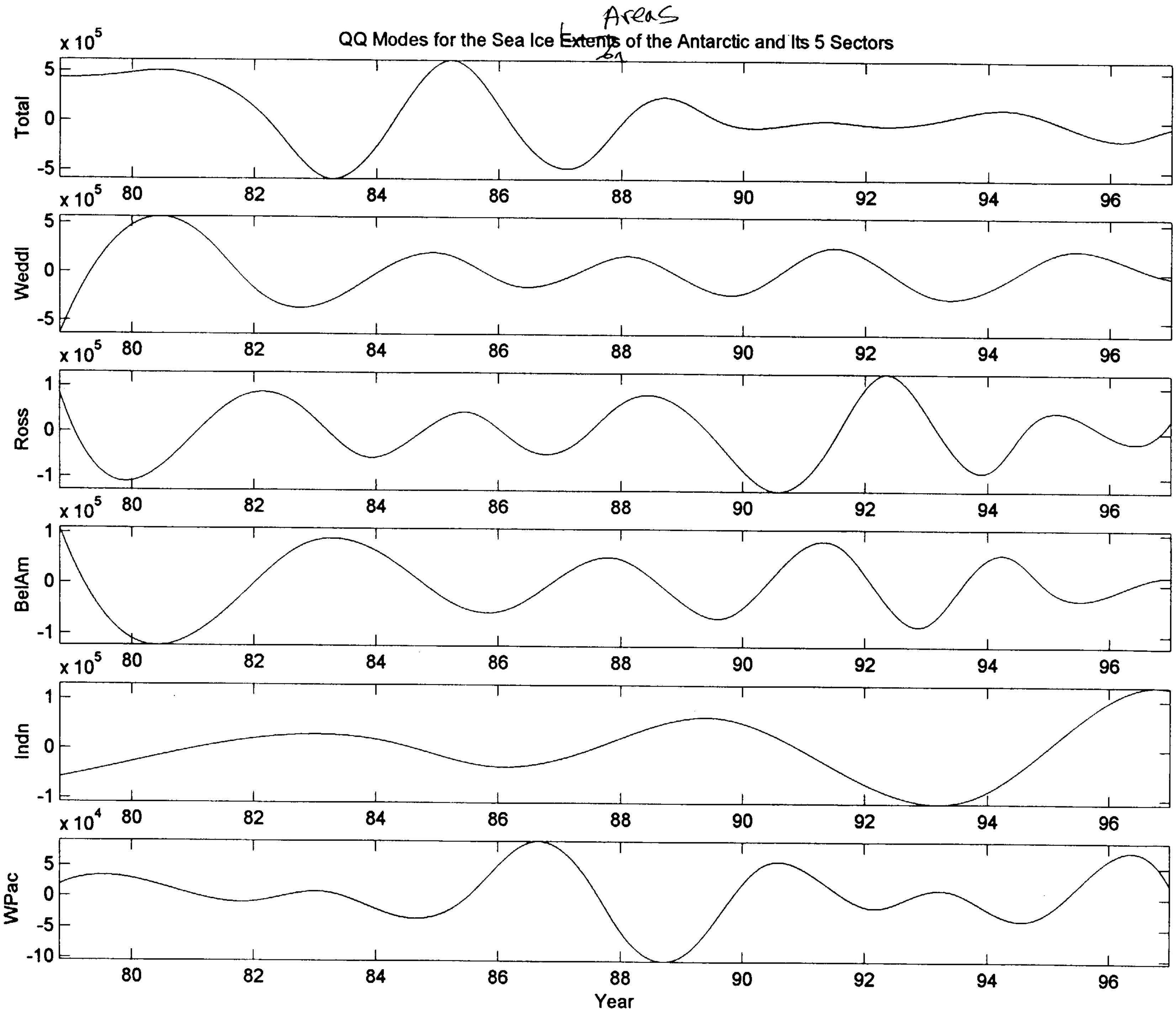

12

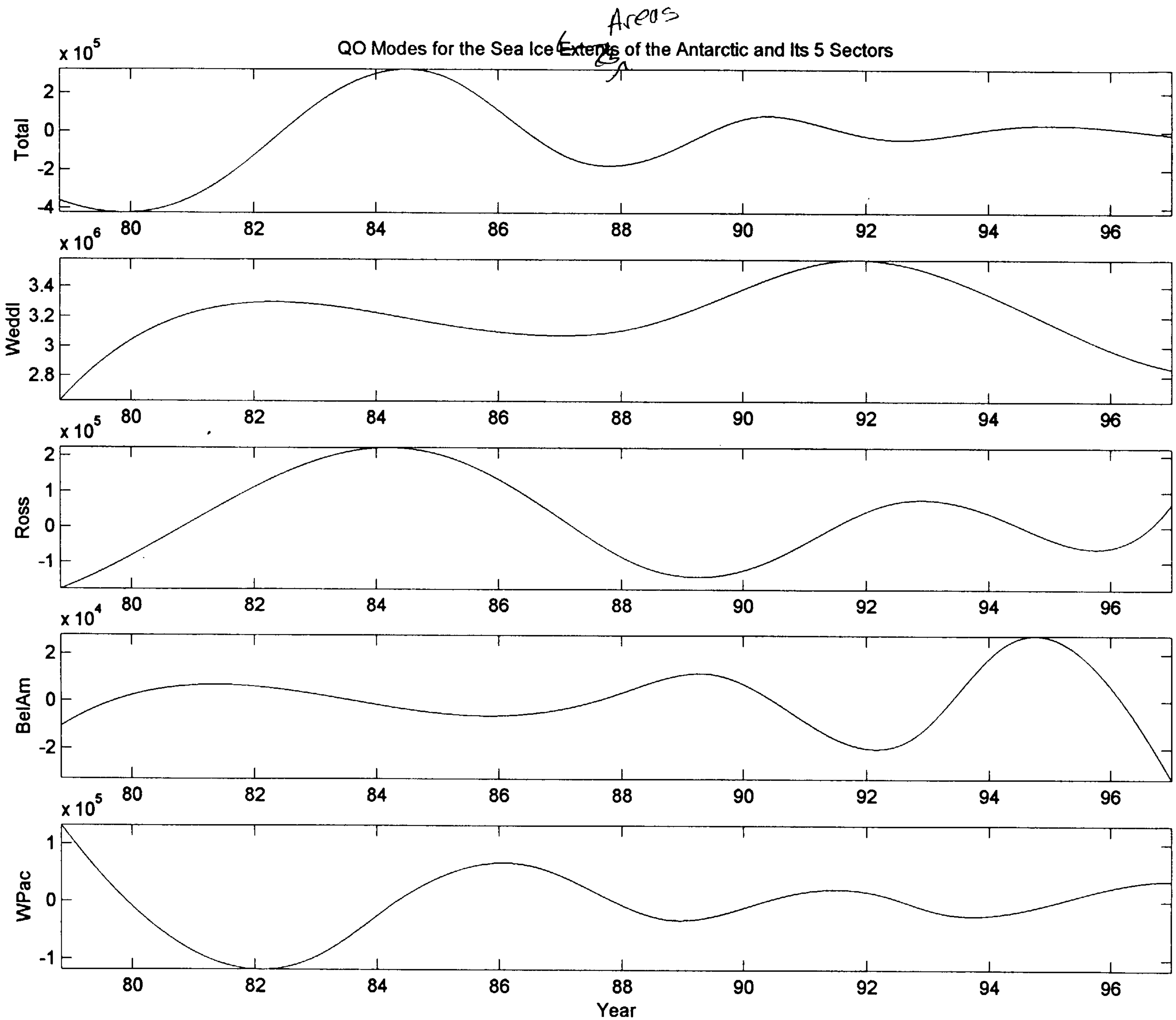

QO Modes for the Sea Ice Extents of the Antarctic and Its 5 Sectors
Areas
x 10^5
Total
2
0
-2
-4
x 10^6
Weddl
3.4
3.2
3
2.8
x 10^5
Ross
2
1
0
-1
x 10^4
BelAm
2
0
-2
x 10^5
WPac
1
0
-1
80
82
84
86
88
90
92
94
96
Year

13

Quasibiennial Modes for the NAO, the SOI, the LOD, and for Global Sea Ice Extents, Areas and Enclosed Open Water

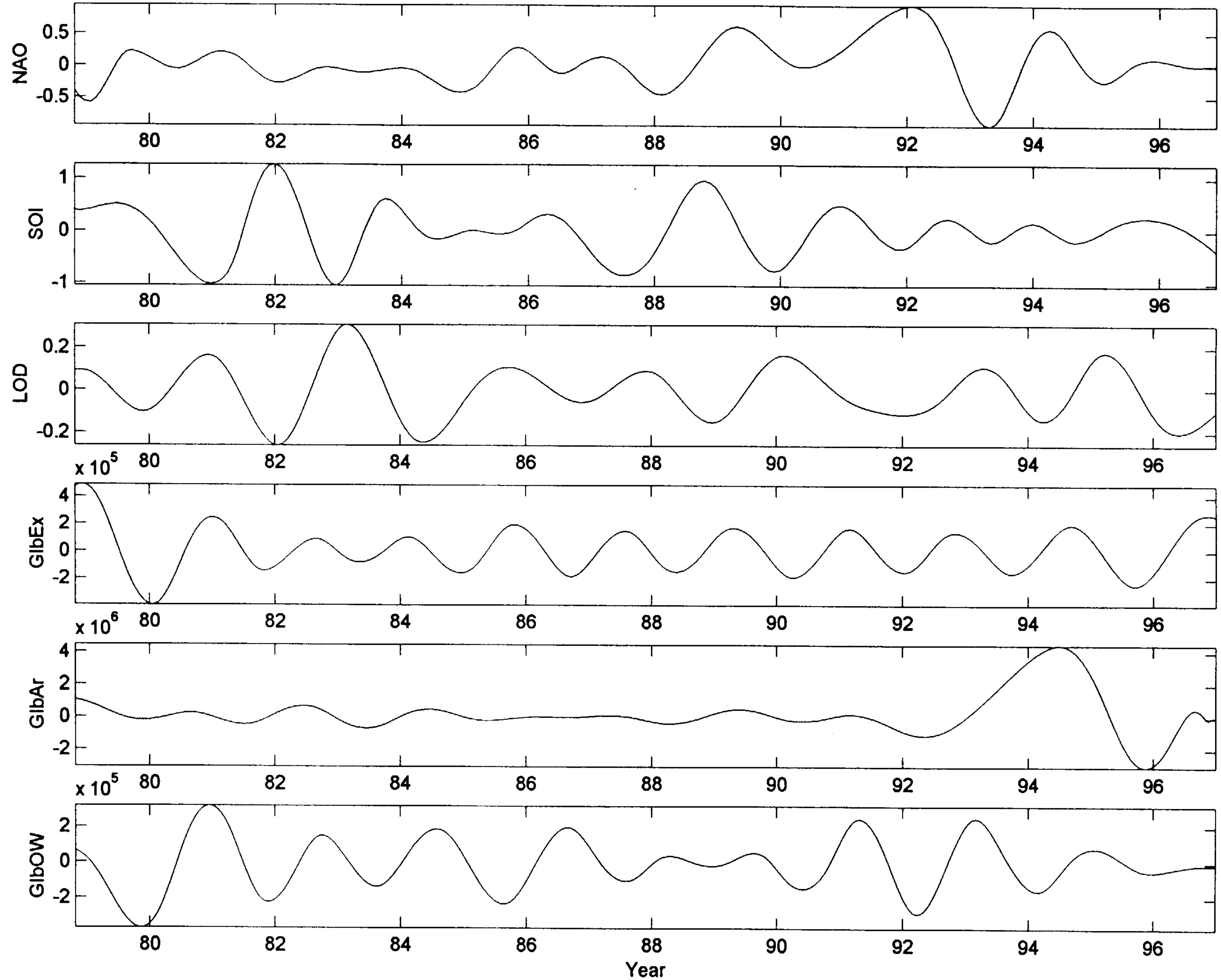

Quasiquadrennial Modes for the NAO, the SOI, the LOD, and for Global Sea Ice Extents, Areas and Enclosed Open Water

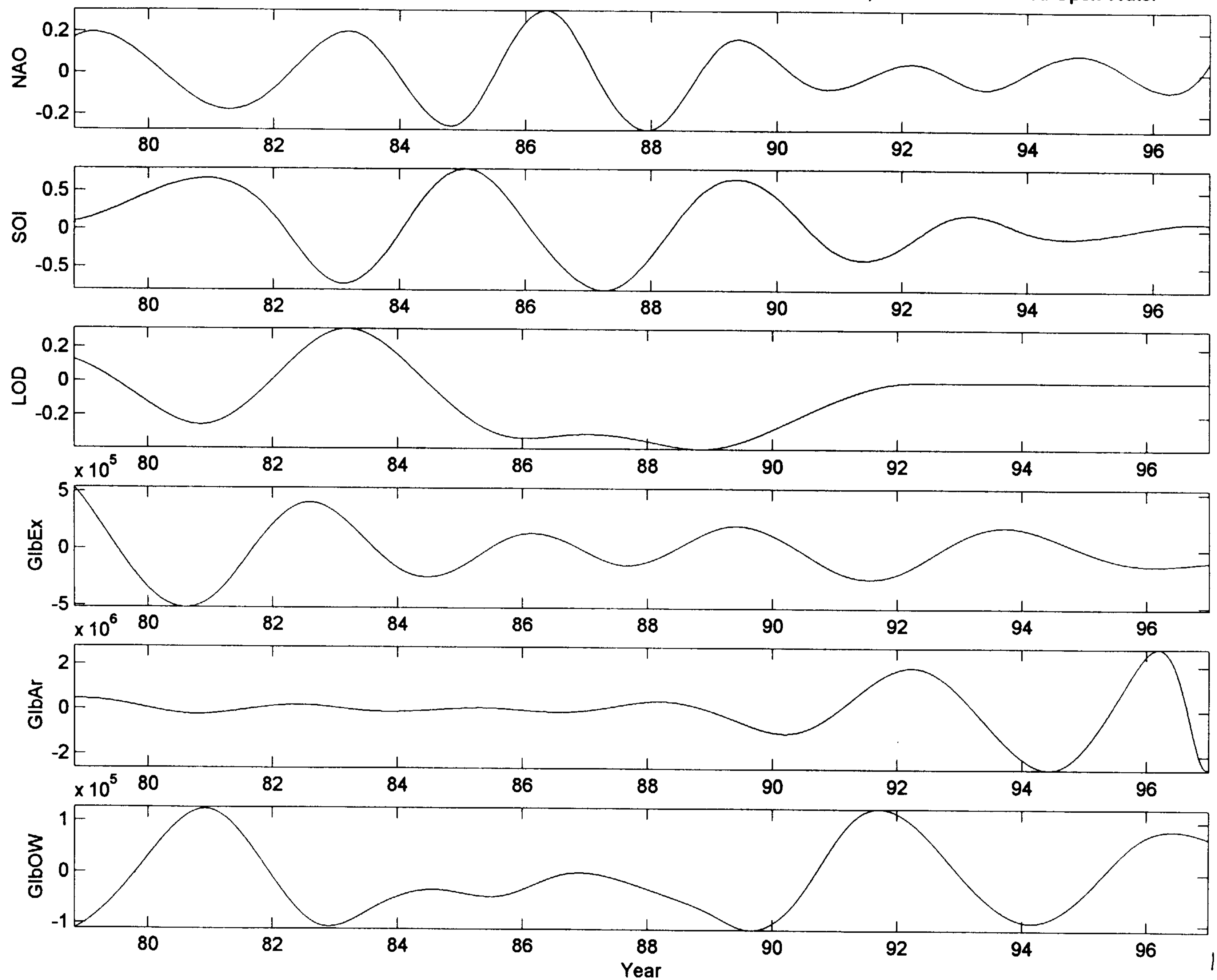

15

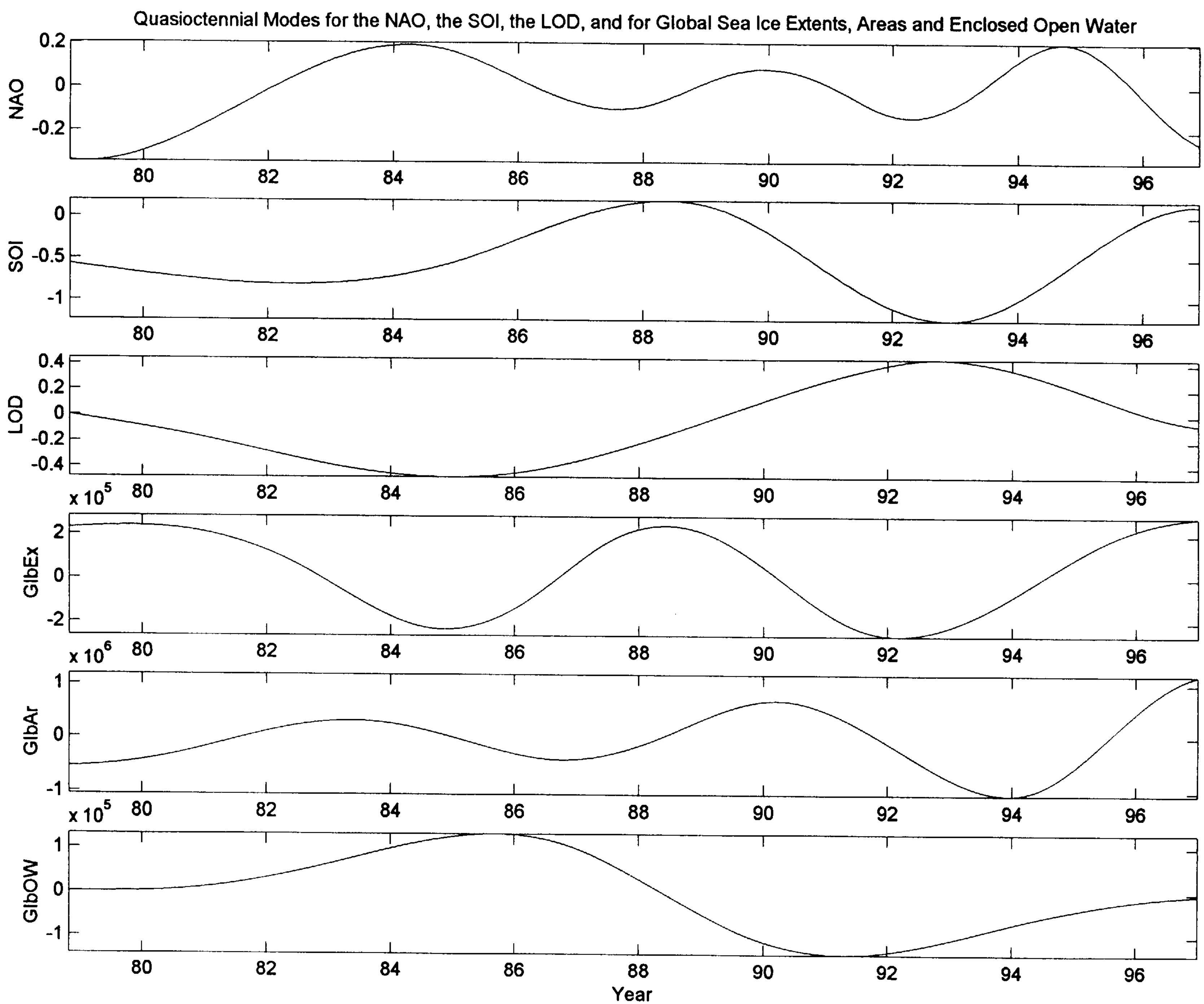

Quasioctennial Modes for the NAO, the SOI, the LOD, and for Global Sea Ice Extents, Areas and Enclosed Open Water
NAO
SOI
LOD
GlbEx
GlbAr
GlbOW
x 10^5
x 10^6
x 10^5
Year
80
82
84
86
88
90
92
94
96